Rock Mechanics
and Rock Engineering 24, 179—206

Rock Mechanics and Rock Engineering

A Constitutive Law for Rock Salt Based on Creep and Relaxation Tests

By

M. Haupt

Philipp Holzmann AG, Technical Department, Frankfurt,
Federal Republic of Germany

Summary

The paper deals with uniaxial relaxation tests on rock salt which are the basis for a constitutive equation. Since so far no regard was paid to relaxation behaviour, corresponding test results are not available and hence a special device for performing of uniaxial relaxation tests had to be constructed. Some interesting test results are discussed in the paper. These results are useful for the verification of constitutive equations. A critical analysis of conventional constitutive laws and their fundamentals shows that these material laws have considerable imperfections and are rested on substantial restrictions. Particularly, they are not able to describe relaxation behaviour sufficiently. Consequently, a constitutive law is proposed consisting of a strain hardening approach with separate creep and relaxation functions. By post-calculation of different laboratory tests it could be shown that in comparison to conventional steady-state creep equations this material law describes the viscous behaviour of rock salt more realistically.

1. Introduction

Due to its high viscosity rock salt in situ always occurs unjointed and hence can be considered as a continuum. In this respect the mathematical formulation of material behaviour is easier than that of most other rocks. On the other hand rock salt shows a very complex rate and temperature dependent behaviour. Despite of this handicap a lot of different constitutive laws have been developed for the description of the viscous behaviour of rock salt. Amongst these theoretical investigations, comprehensive laboratory tests have been performed in recent years. In both cases creep behaviour was the centre point of the research. On the contrary stress relaxation processes were neglected despite of their significant influence on the in situ stress-strain-behaviour.

2. Conventional Constitutive Laws for Rock Salt

Mostly, the strain rates of a rate dependent material are divided into an elastic and a viscous part:

$$\dot{\varepsilon}_{ij} = \dot{\varepsilon}_{ij}^{\mathrm{el}} + \dot{\varepsilon}_{ij}^{\mathrm{vis}} . \tag{1}$$

Usually, the elastic strain rates are assumed to follow Hookes law

$$\dot{\varepsilon}_{ij} = \frac{1}{2G}\,\dot{s}_{ij} + \frac{1}{9K}\,\dot{\sigma}_{kk}\,\delta_{ij}, \tag{2}$$

where G and K denote the shear and the bulk modulus and s_{ij} are the deviatoric stress rates

$$\dot{s}_{ij} = \dot{\sigma}_{ij} - \frac{1}{3}\,\dot{\sigma}_{kk}\,\delta_{ij}. \tag{3}$$

So far, research concentrated upon the viscous part $\dot{\varepsilon}_{ij}^{\mathrm{vis}}$ describing steady-state creep with constant creep rate or transient creep with decreasing creep rate. Tertiary creep followed by creep rupture is not considered here.

Steady-state Creep

If we assume that the material behaviour can be described by the functional link

$$f(\dot{\varepsilon}_{ij}, \sigma_{ij}, T, S_i) = 0, \tag{4}$$

where T denotes the temperature and the state variables S_i characterize the actual microscopic structure, a general constitutive law for the secondary creep of an isotropic incompressible material with multiplicative terms of stress and temperature dependency is given by

$$\dot{\varepsilon}_{ij}^{\mathrm{vis}} = f_1(\sigma_e) \cdot f_2(T)\,\frac{\dot{s}_{ij}}{\sigma_e} \tag{5}$$

with

$$\sigma_e = \sqrt{\frac{1}{2}\left((\sigma_1 - \sigma_2)^2 + (\sigma_2 - \sigma_3)^2 + (\sigma_1 - \sigma_3)^2\right)} . \tag{6}$$

The structure variables S_i are mostly assumed to be constant or to be included in the remaining measuring parameters and therefore do not appear explicitely.

Commonly, the temperature dependency $f_2(T)$ follows the Arrhenius equation

$$f_2(T) = C \exp\left(-\frac{Q}{RT}\right) \tag{7}$$

with the universal gas constant R ($R = 8.314\ \mathrm{J/mol \cdot K}$), an activation energy Q and a positive constant C. The Arrhenius dependency is confirmed by many laboratory tests as well as theoretical investigations.

Steady state creep laws mainly differ in regard to the stress dependent function $f_1(\sigma_e)$. A frequently applied expression is the power dependency

$$f_1(\sigma_e) = C\left(\frac{\sigma_e}{\sigma_0}\right)^n, \quad n \geq 1, \tag{8}$$

where σ_0 denotes a reference stress. A power law for rock salt was proposed by Heard (1972) and accepted by many other authors.

Sometimes the function

$$f_1(\sigma_e) = C_1 \sinh\left(C_2 \frac{\sigma_e}{\sigma_0}\right) \tag{9}$$

is used resulting from Prandtl's theoretical models (Prandtl, 1928) and originally proposed as constitutive law for metals (Nadai, 1928; McVetty, 1943). Both the power law and the hyperbolic sine law can be derived from microstructural considerations as it is shown by Heard (1972).

Transient Creep

Creep deformations with a decreasing creep rate initially being observed in creep tests are generally described by time hardening or strain hardening theory. Time hardening is given if the creep rate depends explicitely on time. In connection with a power approach for the stress and temperature dependency a time hardening law for rock salt as

$$\dot{\varepsilon}_{ij} = C_1 \left(\frac{\sigma_e}{\sigma_0}\right)^{C_2} \left(\frac{T}{T_0}\right)^{C_3} \left(\frac{t}{t_0}\right)^{C_4} \frac{s_{ij}}{\sigma_e} \tag{10}$$

is assumed by Lomenick and Bradshaw (1969) and with similar formulations by e. g. Thoms et al. (1973), Wagner (1982) and Fernandez and Hendron (1984). An exponential time dependency

$$\dot{\varepsilon}_{ij} = C \exp\left(-\frac{t}{t_0}\right) \frac{s_{ij}}{\sigma_e}. \tag{11}$$

is proposed by Wawersik et al. (1984).

An explicite strain dependency of the transient creep deformation leads to a strain hardening law. Menzel and Schreiner (1977) give the following constitutive law for rock salt:

$$\dot{\varepsilon}_{ij} = C^1 \left(\frac{\sigma_e}{\sigma_0}\right)^{C_2} \varepsilon_e^{-C_3} \frac{s_{ij}}{\sigma_e}. \tag{12}$$

This approach is applied to hard salt, too (Menzel and Schreiner, 1975).

Constitutive Laws Derived from Deformation Mechanism Theories

Besides the more empirical approaches, many constitutive laws for rock salt have been established basing on theories of atomic processes in crystal-

line solids. Plastic flow of crystals is caused by lattice defects which are responsible for several deformation mechanisms (see Frost and Ashby, 1982; Poirier, 1985; e. g.). Though these different mechanisms are interacting in complicated ways, in most cases one mechanism is assumed to be dominating. Depending on the normalized deviatoric stress and the

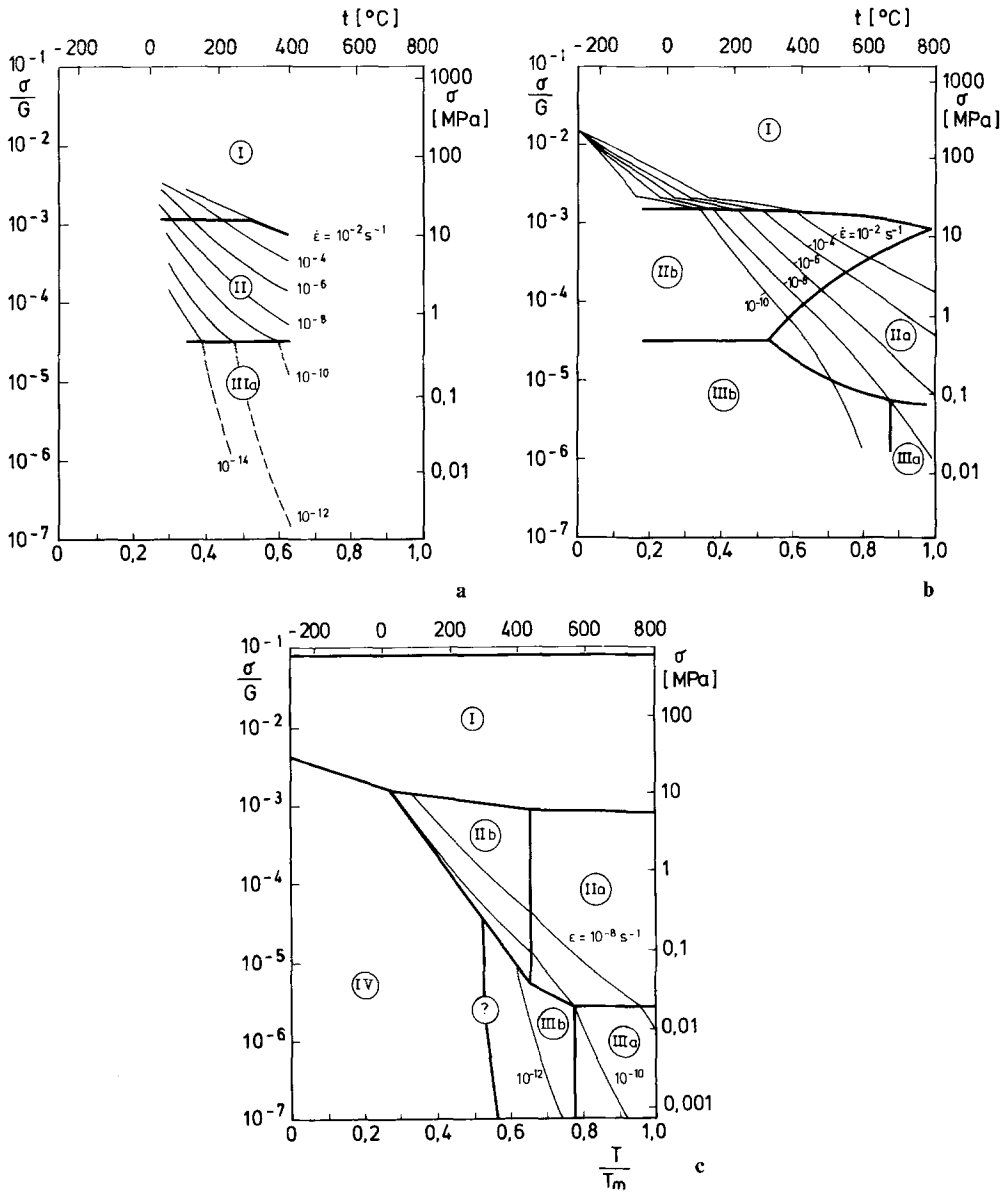

Fig. 1. Deformation-mechanism maps for steady-state creep of rock salt after **a:** Heard (1972), **b:** Verrall et al. (1977) and **c:** Munson/Dawson (1984)
(*G:* Elastic shear modulus, *T:* absolute temperature, T_m: melting temperature)
I: Dislocation glide, II: Dislocation climb, IIa: Volume diffusion, IIb: Pipe diffusion, IIIa: Nabarro-Herring creep, IIIb: Coble creep, IV: Undefined mechanism(s)

homologous temperature, the dominating mechanisms can be presented in so called deformation-mechanism maps as shown in Fig. 1. The boundaries are determined with the aid of laboratory tests on natural and artificial rock salt samples, theoretical models, empirical constitutive laws as well as interpolation and extrapolation.

Without going into details the most important equations basing on microstructural processes should be mentioned. For pure diffusional creep (region III in Fig. 1) we get

$$\dot{\varepsilon} = \frac{\sigma \Omega}{d^2 kT} \left(C_v D_v + C_b \frac{\delta}{d} D_b \right), \tag{13}$$

where Ω denotes the atomic volume, d the grain size, k the Boltzmann-constant and δ the thickness of the boundary. D_v and D_b are the lattice diffusion coefficient and the boundary diffusion coefficient, respectively. In the case of lattice diffusion controlling the creep rate, D_v can be neglected in Eq. (13) (Nabarro-Herring-creep). Correspondingly, C_b is ignored if grain-boundary diffusion dominates (Coble creep).

There are controversial opinions on the mechanism controlling dislocation glide (region I). If the obstruction of the dislocation movement by discrete obstacles is assumed to influence the creep rate primarily (as done by Nicolas and Poirier (1976), e. g.), we obtain:

$$\dot{\varepsilon} = C_1 \left(\frac{\sigma}{G} \right)^n \exp \left[- \frac{\Delta F}{kT} \left(1 - \frac{\sigma}{\sigma_0} \right) \right] \tag{14}$$

with ΔF: activation energy and n, σ_0: constants. When activation energy and/or stress is large, the exponential stress dependency dominates and σ/G is approximately constant. Otherwise the stress rate follows a power law.

If dislocation glide is controlled by lattice resistance (Peierls force) the following equation is valid:

$$\dot{\varepsilon} = C_2 \left(\frac{\sigma}{G} \right)^n \exp \left[- \frac{\Delta F_p}{kT} \left(1 - \left(\frac{\sigma}{\sigma_0} \right)^p \right)^q \right], \tag{15}$$

where ΔF_p denotes the activation energy for overcoming lattice resistance and p and q are constants. Frost and Ashby (1982) and Verrall et al. (1977) give $p = 3/4$, $q = 4/3$, $n = 2$ and Poirier (1985) proposes $p = q = 1$ and $n = 2.5$.

Dislocation climb (region II) is a combination between glide and diffusion processes. Though the strain is caused by dislocation glide the creep rate is diffusion controlled since diffusion proceeds considerably slower than glide. Depending on the main transportation way, dislocation climb is divided in two mechanisms which can be described by

$$\dot{\varepsilon} = \frac{bG}{kT} \left(\frac{\sigma}{G} \right)^n \left[C_1 D_{sd} + C_2 \left(\frac{\sigma}{G} \right)^2 D_c \right], \tag{16}$$

where D_{sd} and D_c is the self-diffusion and the pipe diffusion coefficient, respectively. In proportion as the transport of matter proceeds through the lattice (volume diffusion) or along dislocations (pipe diffusion) the stress exponent becomes n or $(n+2)$ where n is between 3 and 5.

The deformation-mechanism maps show that for practical purposes including conditions of nuclear waste disposal first of all volume diffusion controlled dislocation climb is of importance. Furthermore, dislocation glide or Coble creep may occur.

Amongst extensive investigations on the microstructural background of steady-state creep there are few works dealing with mechanisms causing transient creep. Mott (1953) obtained following solutions:

$$\varepsilon = C_1 \ln (C_2 t + 1) \tag{17}$$

and

$$\varepsilon = C t^{\frac{1}{3}}, \tag{18}$$

which were applied to salt rock by Le Comte (1965) and Höfer and Knoll (1971). Equation (18) coincides with the empirical creep law given by Andrade (1910). Le Comte (1965) shows that the time exponent n can accept values differing from 1/3.

Rheological Models

There are several approaches using rheological models (Serata, 1968; Winkel et al., 1972; e. g.). It seems that with the aid of more or less complicated combinations of three rheological bodies representing the elastic, viscous and plastic properties nearly every rate dependent material behaviour can be described. However, there are decisive restrictions attached to rheological models as it is shown in the following discussion. For this reason a detailed analysis of rheological models for rock salt can be omitted, especially since there exists an extensive bibliography on this subject (Reiner, 1968, e. g.).

Discussion

Constitutive laws for rock salt mostly consist of an additive combination of the elastic Hooke part and a viscous strain rate term which may be written (see Eq. (1)) as:

$$\dot{\varepsilon} = \frac{\dot{\sigma}}{E} + c(\sigma, \varepsilon), \tag{19}$$

where $c\,(\,)$ denotes the creep function. In this case, relaxation behaviour with $\dot{\varepsilon} = 0$ is described by

$$\dot{\sigma} = -E c(\varepsilon, \sigma) = r(\varepsilon, \sigma) \tag{20}$$

with $r\,(\,)$: relaxation function, and the relation between creep and relax-

ation function can be influenced only by the elastic constant E. Accordingly, constitutive laws based on Eq. (19) are very restricted to their flexibility since relaxation behaviour is completely determined by creep behaviour and Young's modulus. Much more flexibility would be given if creep and relaxation function could be determined independently.

In contrast to common assumptions the existence of an elastic part is not necessary for the description of relaxation. In addition, the division of the strain rate into separate parts (Eqs. (1) and (19)) is as unrealistic as the introduction of boundary conditions. According to its definition, a viscous material like rock salt cannot possess a rate independent elastic part. Only for rapid loading and unloading the behaviour is that of a perfectly elastic material. This property is called instantaneous elasticity (see Rivlin, 1970, e. g.). Elastic "constants" E given in literature are rate dependent and accordingly in a strict sense no material parameters.

In an instantaneous elastic material elastic and viscous strains appear at the same time and are not combined with an exceeding of a boundary condition. It should be pointed out that the postulate of two strain rate parts operating in different intensity and influencing each other, is not based on an experimentally provable physical process but has to be understood as a mental conception. In the microstructure of rock salt separately operating elastic and viscous mechanisms cannot be found.

The assumption of the existence of a discrete elastic part is caused by rheological models for the most part since these models always suppose separate mechanisms for elastic, viscous and plastic behaviour. Since the properties of these three basic models do not exist separately in a real material, rheological models never reproduce the structure of a material. They are abstract.

Rheological models exhibit a lot of disadvantages. Their applicability is limited on uniaxial mechanical behaviour since conventional models are not able to describe threedimensional material behaviour as well as non-mechanical effects. On account of the additive superimposition of the stress or strain parts, the activation of these parts has to be combined with boundary conditions without continuous transitions being possible. Moreover, the application of rheological models often leads to exponential terms which do not allow a sufficient approximation of the real salt rock behaviour.

To avoid these disadvantages non-linear rheological elements are used. In this case the corresponding equations may become very complicated and obviously, several of these approaches were never applied. Moreover, the main advantage of the models — the clear graphical illustration of mutually influencing mechanical processes — gets lost. Considering the restricted applicability and other disadvantages, the suitability of rheological models as a basis for the development of constitutive laws for rock salt seems to be rather doubtful.

Another group of constitutive laws proves to be incorrect. Time dependent laws like the time hardening approach (Eqs. (10) and (11)) are always imperfect material descriptions inasmuch as explicite time depen-

dency indicates that the physical origin of the time dependency is unknown (Becker and Bürger, 1975). Time does not influence strain or stress causes and is no independent state variable which for instance can be held constant (McCartney, 1976). Besides, Odqvist and Hult (1962) point out that the time hardening theory shows poor agreement with experimental results in case of rapid stress changes. Hence, explicite time dependency should be avoided in constitutive laws.

The knowledge of the microstructural deformation mechanisms seems to be the best basis for the description and extrapolation of material behaviour. However, micromechanical theories also show many insufficiencies which are often underestimated. First indication of the difficulties is given by the fact that according to the underlying assumptions, a considerable variety of partly conflicting approaches can be derived from these theories.

The distinction of different deformation mechanisms limits the practical applicability of the micromechanical theories inasmuch as the description of stress or strain changes requires several equations whose validity must be ascertained by limit conditions. Particularly, this problem occurs at the simulation of a relaxation test, since related to the deformation mechanism map, relaxation is no state but a process which may pass several deformation mechanisms.

With the exception of distinct lattice defects, other structural anomalies and obstructions are not considered by micromechanical theories. Impurities which are always found in natural rock salt and which decisively may influence the mechanical behaviour are included just as little as nonmechanical processes and other effects such as microcracks. Since due to the complicated interactions the complete deformation process cannot be described in a theoretical model, only one mechanism is considered in each case which is assumed to be dominating.

As shown above, micromechanical theories are based on the assumption of a constant structure. For instance, Orowan's equation

$$\dot{\varepsilon} = C \rho_m b v, \tag{21}$$

where ρ_m, b and v denote the density of the mobile dislocations, the Burgers vector and the average velocity of the dislocations respectively, is valid only for constant dislocation density which is given approximately for steady-state creep. In view of the fact that on the one hand this microscopic constitutive equation lies at the basis of most equations describing the various deformation processes (Poirier, 1985) and on the other hand in situ the dislocation density continuously changes due to stress redistributions and other circumstances, it becomes evident that the applicability of the corresponding equations is strongly limited. Yet mostly the fundamental assumption of constant structure is not taken into account by applying steady-state creep equations to relaxation processes.

These disadvantages do not apply to phenomenological constitutive laws. Phenomenological or empirical approaches are not based on any the-

oretical structure model and hence need not the corresponding simplifications but consider the material as it is found in nature including impurities and nonmechanical processes.

3. Experimental Procedure

The stress-strain-behaviour in situ is influenced by creep and relaxation processes likewise. In contrast to creep, relaxation behaviour of rock salt has hardly been tested up to now. For this reason a new relaxation testing equipment had to be developed. In addition, uniaxial creep tests were performed.

It has to be remarked that uniaxial relaxation tests are characterized by approximately constant axial deformation. Due to stress measurements a very small axial deformation always has to be admitted. Lateral deformations have to be allowed also. Otherwise, uniaxial relaxation tests whould be possible only at a material with constant volume.

The tested natural rock salt originates from a northern German rock salt mine from a depth of about 700 m and exhibits a high purity of more than 98 per cent. It is a polycrystalline, almost monomineral salt without showing anisotropy. The average grain diameter is about 10 mm.

The cylindrical samples were prepared on a special facing lathe ensuring a tolerance of 0.5 μm concerning the parallelism of the faces. There were samples used with a diameter d of 54 mm and a height h ranging from 108 to 135 mm. The ratio h/d amounted between 2.0 and 2.5.

Relaxation Tests

For carrying out uniaxial relaxation tests, a special relaxation device was developed at the Institute of Soil and Rock Mechanics of the University of Karlsruhe (Balthasar et al., 1987). The apparatus consists of a four-column load frame with a screw jack which is driven by an electric motor (Fig. 2). A reduction gear serves to move the screw jack for fitting the sample in and out. The screw jack is supplied with a built-in electronic load cell.

The two main problems in constructing a relaxation device are the regulation of the axial deformation and the elimination of the temperature effect. Since it is impossible to construct a load frame holding the deformation constant on account of its stiffness alone, a regulation of the axial strain is inevitable. For this reason, the relaxation device was applied with a digital strain gauge with a resolution of 1 μm measuring the distance between the loading plates. This strain gauge is connected with a self-developed microprocessor-supported closed loop control system which ensures a maximum deviation of the nominal deformation of 0.5 μm.

In most tests the lateral strain was measured by a special measuring clip (Haupt, 1988). Axial force and lateral strain were recorded continuously by an *Y-t*-recorder.

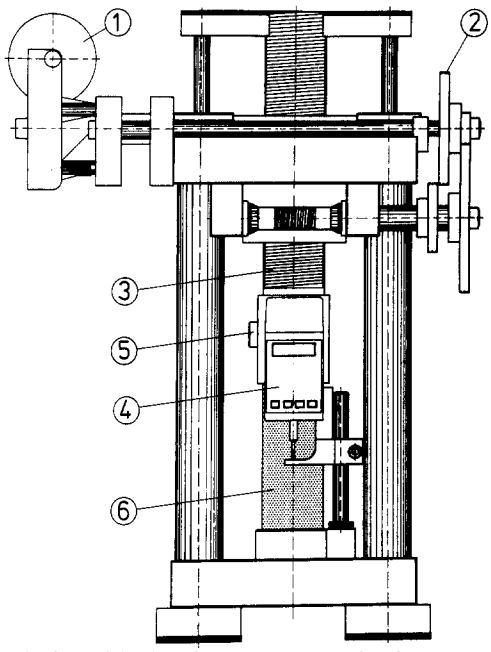

Fig. 2. Relaxation device: *(1)* Electric motor, *(2)* reduction gear, *(3)* screw jack, *(4)* digital strain gauge, *(5)* load cell, *(6)* specimen

Preliminary tests showed a huge impairment of the relaxation behaviour by the temperature (Fig. 3) which could not be essentially reduced by applying an isolation. The temperature deviation had to be much lower than 1 *K*. On this account, the whole testing apparatus was placed within a temperature controlled box ensuring temperature deviations of 0.1 *K* maximum.

The relaxation tests were performed at a temperature of 35.0 °C and at four different strain levels ($10^3 \cdot \varepsilon = 5$, 10, 15 and 20). Loading and unloading was brought in with a constant strain rate of about $4 \cdot 10^{-5}$/s. Results of more than 30 relaxation tests are available. The tests lasted between one hour to 132 days.

Creep Tests

Since the main subject of this work deals with relaxation behaviour, the procedure and the results of creep tests will be described abbreviated. For the performance of uniaxial creep tests two different test devices were used. First tests were carried out in a conventional hydraulic test apparatus supplied with a special appliance for ensuring constant stress. To raise capacity, a simple hydraulic creep test device was developed consisting of two four-column load frames which are connected by one hydraulic system. This construction allows carrying out two tests simultaneously. Constant stress was provided by a nitrogen-buffered pressure balance reservoir.

Stress deviations never exceeded 0.5 percent of the nominal value. For elimination of tipping effects every testing-stand was supplied with three mechanical strain gauges.

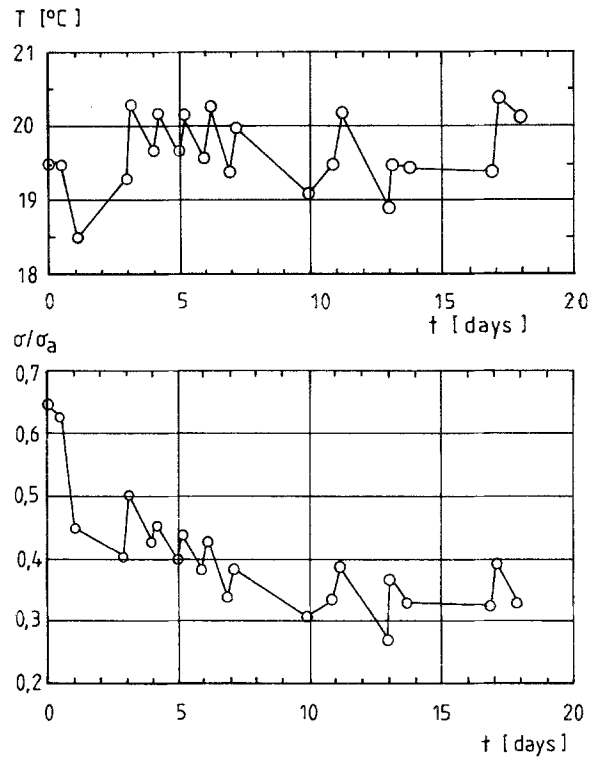

Fig. 3. Temperature effect on relaxation behaviour measured in preliminary tests

Creep tests were performed at ambient temperatures. Ten samples were used with altogether 26 creep phases at stresses of 5, 10, 15 and 20 MPa. The tests lasted between 13 and 95 days.

4. Experimental Results

Relaxation Tests

The time dependent relaxation behaviour is evaluated with the aid of diagrams with a logarithmic time scale. Graphs with a linear time scale do not permit any conclusive extrapolations and hence are completely unsuitable for a scientific evaluation. This concerns creep tests, too, and there are numerous misinterpretations in literature caused by linear time representations.

Figure 4 shows the time dependent dimensionless stress σ/σ_a, where σ_a is the initial relaxation stress which likewise is the maximum stress. Immediately after stopping the loading a very strong stress decrease could be observed. Within only one minute the stress diminished by more than 20 percent, sometimes more than 40 percent. The stress decreases monotonously.

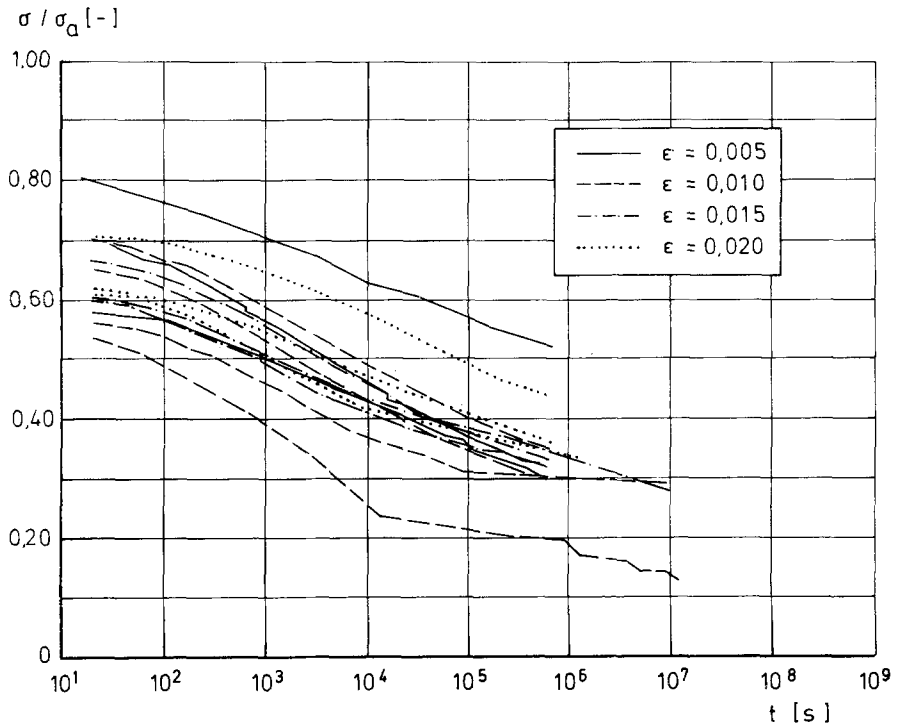

Fig. 4. Relaxation tests: dimensionless stress vs. time

The curves in Fig. 4 show a fairly uniform gradient whereas the scatter is considerable. But certainly, most of the curves are within a $0.1\,\sigma/\sigma_a$ range. No systematic relationship between the strain and the position of the curves can be found. Hence, the relative stress decrease is approximately independent of the strain and the initial stress.

Based on the time dependent stress, the stress rates were calculated as $\dot{\sigma} = \Delta\sigma/\Delta t$, where the time increments Δt were between some minutes and a few days. Since $\Delta\sigma$ is very low at small stress rates, even negligible measuring inaccuracies or strain variations have considerable consequences for the stress rate and lead to a clear deviation. On account of this, the time dependent stress rates exhibit a remarkable conformity (Fig. 5). Obviously, the stress rates are independent of the strain. A "steady-state relaxation", i. e. relaxation with a constant stress rate, can not be observed. The curves can be approximated by a straight line and hence follow a power approach.

As shown by Haupt (1988) relaxation tests allow conclusions about the creep limit much better than creep tests. The creep limit is characterized by the conditions $\dot{\varepsilon} = 0$ and $\dot{\sigma} = 0$ and separates elastic from viscous behaviour. In a relaxation test defined by $\dot{\varepsilon} = 0$, the creep limit is reached when the stress remains constant. Regarding Figs. 4 and 5 it can be ascertained that in no case the creep limit was encountered.

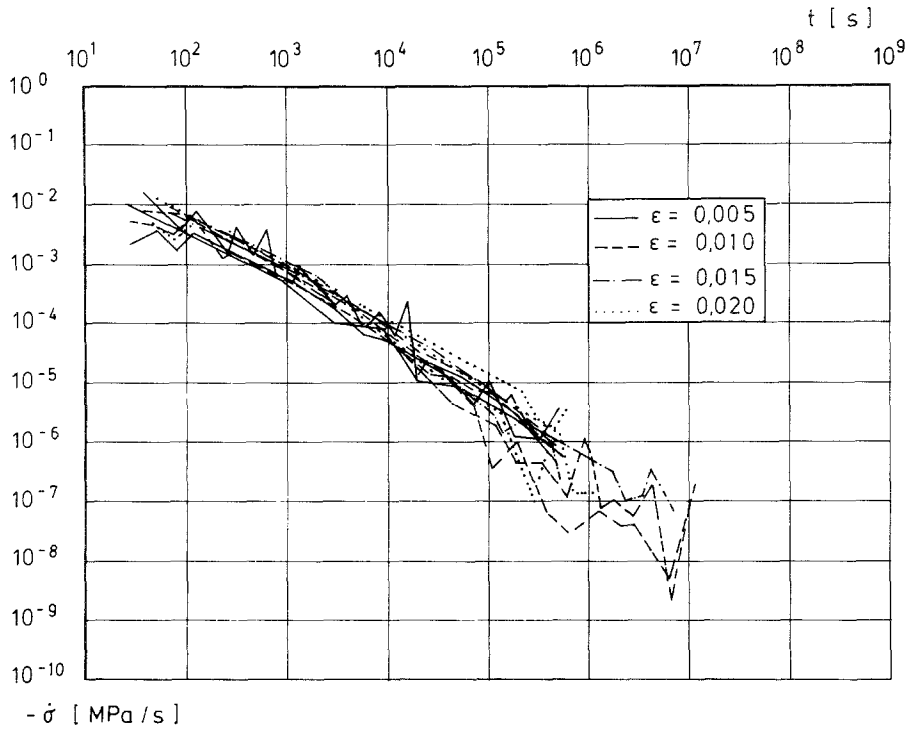

Fig. 5. Relaxation tests: stress rate vs. time

Figure 6 shows the relaxation curves in a σ-ε-diagram in comparison with a creep limit of rock salt given by Dreyer (1967). It becomes evident that the creep limit must be considerably lower than the limit proposed by Dreyer which is based on tests with so called quasistatic loading. Since the relaxation phases were discontinued without any indication of reaching a constant stress level, it is assumed that the creep limit of rock salt is zero. This means that the behaviour is rate dependent even at very low stresses and consequently a relaxation test would terminate in a stress-free state.

Normally every sample was used for only one relaxation test but there were a few tests performed with several relaxation phases. One typical curve is shown in Fig. 7. After discontinuation of the relaxation phases the reloading curves always turn into the fictitious virgin stress strain curve. As demonstrated by some tests, no difference can be perceived between reloading following total unloading after relaxation and reloading following the relaxation process directly without unloading. Relaxation phases do not have any effect on the stress strain curve.

Immediately at the beginning of the relaxation a 1—3 percent increase of the transverse strain was observed. After a rapid retardation of this process the deformations turned back and partly reached negative values. However, this must not be compulsorily an indication of volume contraction. Since the transverse strain is measured only at half height of the sample, the negative transverse strain may be caused by pure change of the

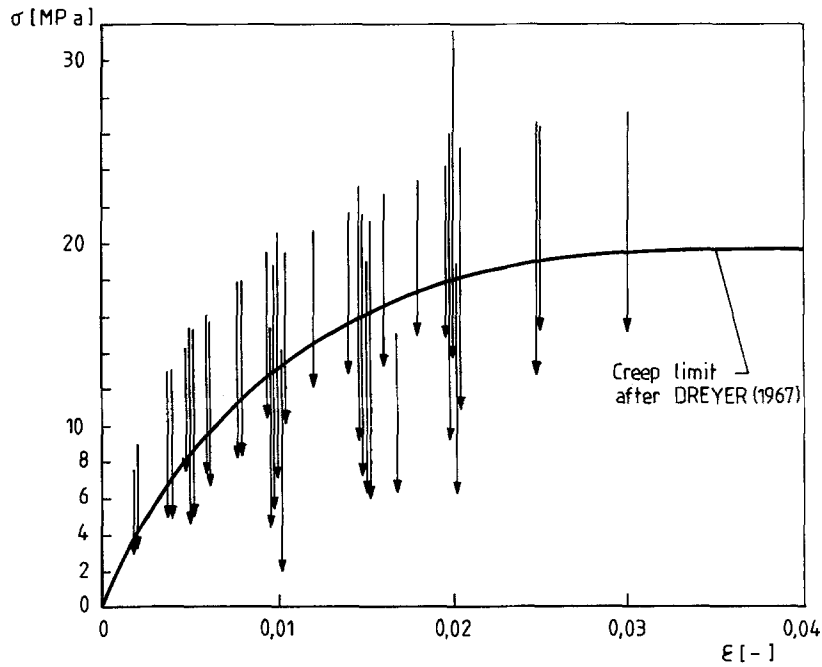

Fig. 6. Creep limit after Dreyer (1967) compared with the relaxation tests

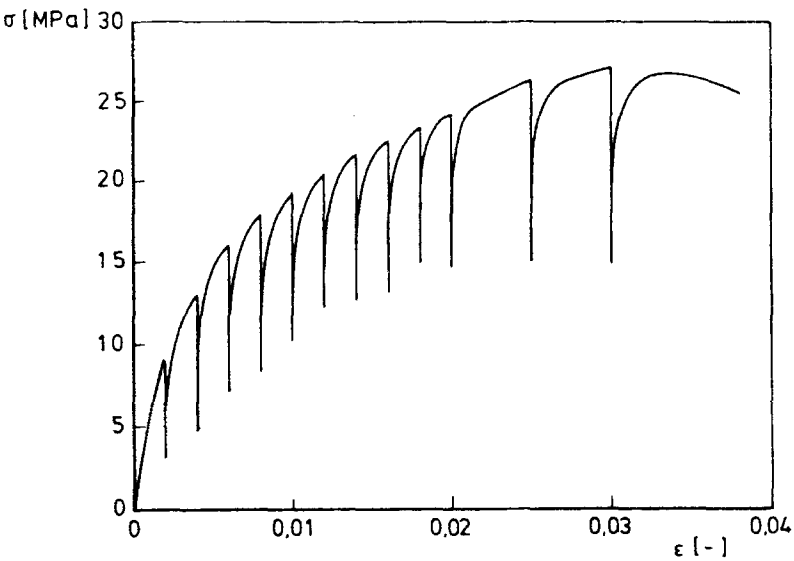

Fig. 7. Typical stress-strain curve of a test with several relaxation phases (duration of relaxation phases between 1 hour and 9 days)

shape in that the bulge of the sample forms back with increasing lateral strains at the upper and lower surface. In consideration of the small transverse strains which only once exceeded 4 percent, it is assumed that stress relaxation of rock salt occurs with constant volume.

Creep Tests

An essential point of discussion is the question whether salt rock has a steady-state creep phase or not. In a strict sense steady-state creep is denoted as a flow with a constant strain rate which is stable and will never end (Poirier, 1985). To simplify matters we will include the so called quasi-steady-state creep which means creep with a minimum strain rate.

As mentioned before, a steady-state regime cannot be proven by a linear ε-t-representation due to time scale effect. Figure 8 exemplarily shows the $\dot{\varepsilon}$-t-curves of four creep tests under a stress of 20 MPa in a bilogarithmic diagram. Obviously, the best approximation would be a straight line. This indicates a power law relation between strain rate and time. The most important point is that a steady-state creep could not be observed in spite of test durations of partly more than 200 days.

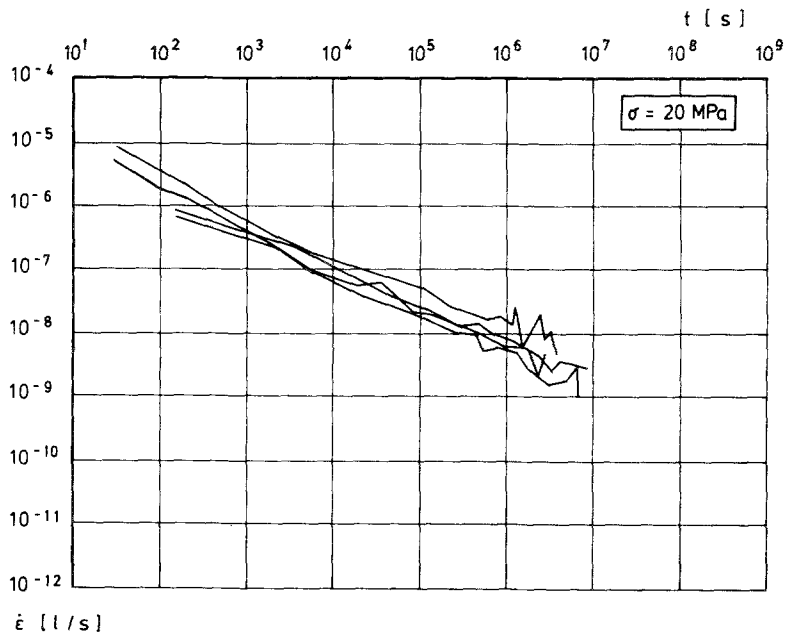

Fig. 8. Creep tests: strain rate vs. time

This agrees with observations made by Lomenick and Bradshaw (1969), where a continuously decreasing creep rate was measured even after more than 3½ years. Due to the immense importance which is attributed to steady-state creep not only in scientific investigations but also in engineering practice, these results deserve particular attention. The assumption of steady-state creep may be an admissible simplification with the object of confining arithmetical problems for instance. However, in publications the approximative nature of given test results and parameters is mentioned very rarely and hence the impression arises that undoubtedly

constant creep rates were measured regularly. As shown exemplarily by Haupt (1988), this is not the case. An impressive confirmation is given by Wawersik (1985), who reports on investigations about the dependency of so called steady-state creep rates upon test duration. It could be ascertained that the strain rate denoted as steady-state creep rate decreases with increasing test duration. This demonstrates that the determination of a steady-state creep rate based on creep tests is very problematic and that creep deformations are overestimated in most cases.

5. Constitutive Law

Basing on the theoretical investigations and in consideration of experimental tests as well as corresponding published works, the following constitutive law for rock salt is proposed:

$$\frac{\dot{\varepsilon}_{ij}}{c\,(\sigma_e, \varepsilon_e)} = \frac{s_{ij}}{\sigma_0} + \frac{\dot{s}_{ij}}{r\,(\sigma_e, \varepsilon_e)}, \tag{22}$$

where

$$c\,(\,) = \frac{3}{2}\,\alpha\,\varepsilon_e^{-\beta}\left(\frac{\sigma_e}{\sigma_0}\right)^{\delta-1} \tag{23}$$

is the creep function and

$$r\,(\,) = A\,\varepsilon_e^{-B}\left(\frac{\sigma_e}{\sigma_0}\right)^{D-1} \tag{24}$$

is the relaxation function. The variable σ_0 is a reference value which is chosen as $\sigma_0 = 1$ MPa. The constitutive law is linear in the rates of strain and stress but nonlinear in the strain and in the stress. Since the approach uses total strains, the determination of boundary conditions is not necessary. Temperature dependency is not included because corresponding tests were not performed. Moreover, the influence of confining stress could not be investigated.

The decisive advantage against constitutive laws according to Eq. (19) lies in the possibility to chose separate creep and relaxation approaches (Eqs. (23) and (24)) independently of each other. By using suitable creep and relaxation functions as also material parameters, many conventional constitutive laws can be deduced from Eq. (22). For rock salt the stress and strain dependent functions according to Eqs. (23) and (24) are chosen which will be proved by analytical simulation of the laboratory tests.

If $\beta = B$, $\delta = D$ and $A/\alpha = E$, the constitutive law reduces to a strain hardening law with an additive elastic strain rate. In this case the viscous strain rate agrees with that of Menzel and Schreiner (1977), (Eq. (12)). If in addition $\beta = B = 0$ is valid, a power law for steady-state creep is obtained. Hence, by Eq. (22) a very general formulation was found which represents a big class of conventional constitutive laws being able to describe both steady-state creep and as transient creep.

Equation (22) agrees with a constitutive law for metals proposed by Krempl and his co-workers (Cernocky and Krempl, 1979; Liu and Krempl, 1979; Cernocky and Krempl, 1980; e. g.), so far as Krempl's function $g(\varepsilon)$ which means the creep limit, is neglected. However, Krempl's law incorporates an elastic part since always a constant relation between creep and relaxation function is assumed: $r(\,)/c(\,) = E$. In addition, with $g(\varepsilon)=0$ creep and relaxation function are merely dependent upon σ allowing no strain hardening approaches for instance.

By inserting Eqs. (23) and (24) into Eq. (22) the following equations are obtained for creep with $\dot{s}_{ij}=0$ and $\sigma_e=\text{const.}$:

$$\dot{\varepsilon}_{ij} = c(\,)\frac{s_{ij}}{\sigma_0} = \frac{3}{2}\alpha\,\varepsilon_e^{-\beta}\left(\frac{\sigma_e}{\sigma_0}\right)^{\delta-1}\frac{s_{ij}}{\sigma_0}; \tag{25}$$

and for relaxation with $\dot{\varepsilon}_{ij}=0$ and $\varepsilon_e=\text{const.}$:

$$\dot{s}_{ij} = r(\,)\frac{s_{ij}}{\sigma_0} = -A\,\varepsilon_e^{-B}\left(\frac{\sigma_e}{\sigma_0}\right)^{D-1}\frac{s_{ij}}{\sigma_0}. \tag{26}$$

In the following uniaxial behaviour will be regarded. Due to $\sigma_e=\sigma_1$, $\varepsilon_e=\varepsilon_1$ and $s_1=\frac{2}{3}\sigma_1$ the constitutive law can be written as

$$\frac{\varepsilon_1^{\beta}}{\alpha}\left(\frac{\sigma_1}{\sigma_0}\right)^{-\delta}\dot{\varepsilon}_1 = 1 + \frac{\varepsilon_1^{B}}{A}\left(\frac{\sigma_1}{\sigma_0}\right)^{-D}\dot{\sigma}_1. \tag{27}$$

Uniaxial creep with $\dot{\sigma}_1=0$ is described by

$$\dot{\varepsilon}_1 = \alpha\,\varepsilon_1^{-\beta}\left(\frac{\sigma_1}{\sigma_0}\right)^{\delta}. \tag{28}$$

Using the creep time

$$t_c = \left[\frac{\alpha(\beta+1)}{\varepsilon_a^{\beta+1}}\left(\frac{\sigma_1}{\sigma_0}\right)^{\delta}\right]^{-1} \tag{29}$$

integration of Eq. (27) with respect to time and the initial condition $\varepsilon_1(t=t_0)=\varepsilon_a$ yields the time dependent creep

$$\varepsilon_1 = \varepsilon_a\left[\frac{(t-t_0)}{t_c}+1\right]^{\frac{1}{\beta+1}} \tag{30}$$

and the time dependent creep rate

$$\dot{\varepsilon}_1 = \frac{\varepsilon_a}{(\beta+1)\,t_c}\left[\frac{(t-t_0)}{t_c}+1\right]^{-\frac{\beta}{\beta+1}}. \tag{31}$$

Correspondingly, relaxation behaviour with $\dot{\varepsilon}_1=0$ is described by

$$\dot{\sigma}_1 = -A\,\varepsilon_1^{-B}\left(\frac{\sigma_1}{\sigma_0}\right)^{D}. \tag{32}$$

With the relaxation time

$$t_r = \left[(D-1) \frac{A}{\sigma_a} \varepsilon_1^{-B} \left(\frac{\sigma_a}{\sigma_0} \right)^D \right]^{-1} \tag{33}$$

the time dependent relaxation is obtained as

$$\sigma_1 = \sigma_a \left[\frac{(t-t_0)}{t_r} + 1 \right]^{\frac{1}{1-D}} \tag{34}$$

and the relaxation rate becomes

$$\dot{\sigma}_1 = \frac{\sigma_a}{(1-D)\, t_r} \left[\frac{(t-t_0)}{t_r} + 1 \right]^{\frac{D}{1-D}} \tag{35}$$

where $D > 1$. If $D = 1$, the time dependency of stress and stress rate is exponential.

Since the relaxation rate as well as the stress decrease monotonously against zero, a completely relaxing material without creep limit is described by the constitutive law.

The constitutive law incorporates six material parameters. A, B and D are determined by relaxation tests, α, β and δ by creep tests as it will be shown in the following.

6. Determination of Material Parameters

In order to enable a comparison between different approaches, material parameters are determined not only for the proposed strain hardening law but also for two conventional steady-state creep laws. For this purpose the power law (Eq. (8)) and the hyperbolic sine law (Eq. (9)) are used because they are very common in practice. Certainly, recent advances led to more sophisticated models being able to characterize creep and relaxation as well as transient and hardening processes. However, due to their complicated mathematical formulation and their restricted range of application these laws are not utilized for a comparison.

Strain Hardening Law

The determination of relaxation parameters for the strain hardening law is done on the basis of Eq. (32) which can be written as

$$\log(-\dot{\sigma}) = \log(A\, \varepsilon^{-B}) + D \log\left(\frac{\sigma}{\sigma_0} \right). \tag{36}$$

This equation represents a straight line in a bilogarithmic $(-\dot{\sigma}) - (\sigma/\sigma_0)$-diagram, from which the parameter D can be derived as the gradient. Considering the corresponding test results (Fig. 9) it can be ascertained that the

gradients of the experimental curves behave rather homogeneously whereas their position differs clearly. Hence, D can be given fairly exact. For determination of A and B first the experimental curves are approximated

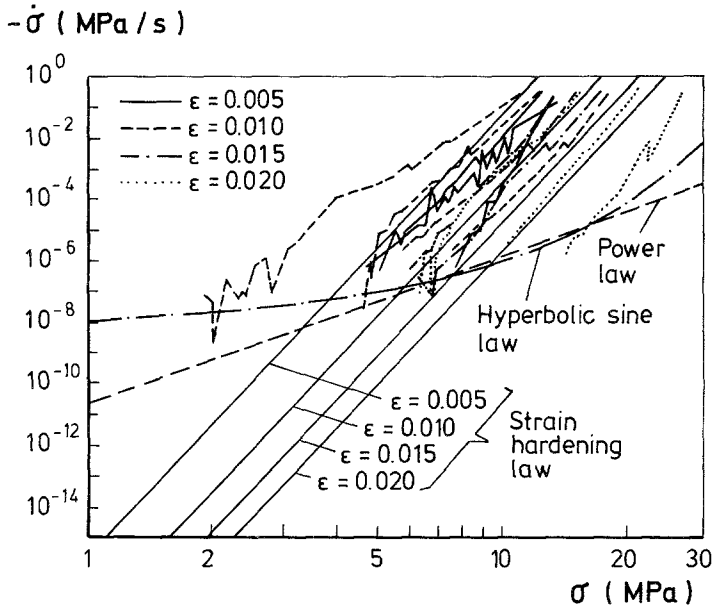

Fig. 9. Stress rate vs. stress: comparison of measured results and theoretical predictions

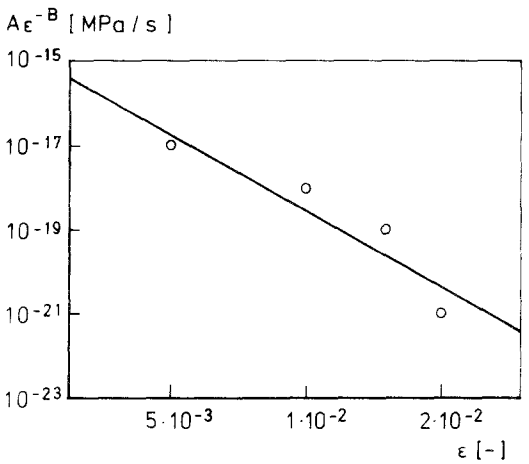

Fig. 10. Diagram for determination of relaxation parameters A and B

by four straight lines to obtain four intercepts of the ordinate at $\log(\sigma/\sigma_0) = 0$ depending on the strain ε. Subsequently, these values which are adequate to $A\varepsilon^{-B}$ are plotted in dependency upon ε. Since this relation like-

wise can be approximated by a straight line in a bilogarithmic graph (Fig. 10), B is obtained as the gradient and A as the intercept of the ordinate. The so determined parameters are: $A = 10^{-33}$ MPa/s, $B = 7.5$ and $D = 15.0$.

The creep parameters α, β and δ are determined similarly. Due to scatter of the creep curves β can be chosen as $\beta = B = 7.5$. The other values are: $\alpha = 6.5 \cdot 10^{-41}$/s and $\delta = 16.5$. The rather small difference between $D = 15.0$ and $\delta = 16.5$ gives reason for the presumption that a further reduction of the constitutive law is possible by using $D = d$. Indeed, the material parameters

$$\begin{aligned} A &= 3 \cdot 10^{-31}\ \text{MPa/s} & \alpha &= 2 \cdot 10^{-36}/\text{s} \\ B &= 6.0 & \beta &= 6.0 \\ D &= 15.0 & \delta &= 15.0 \end{aligned}$$

show satisfactory agreement with experimental results. The corresponding calculated curves are depicted in Figs. 9 and 10.

Due to $B = \beta$, $D = \delta$ and hence

$$\frac{c()}{r()} = -\frac{3\alpha}{2A} \tag{37}$$

the uniaxial constitutive law reduces to

$$\dot{\varepsilon} = \frac{\alpha}{A}\dot{\sigma} + \frac{2}{3}c()\frac{\sigma}{\sigma_0}. \tag{38}$$

This equation formally is adequate to the strain hardening approach with elastic part (Eq. (12)). It has to be pointed out that the reduced equation (Eq. (38)) is valid only for the rock salt investigated here. Generally, Eq. (22) should be applied. It may be possible that the simplification according to Eq. (38) cannot be maintained if increased precision is required.

Power Law

In case of uniaxial creep the power law

$$\dot{\varepsilon} = \frac{\dot{\sigma}}{E} + A^p\left(\frac{\sigma}{\sigma_0}\right)^n \tag{39}$$

reduces to

$$\dot{\varepsilon} = A^p\left(\frac{\sigma}{\sigma_0}\right)^n. \tag{40}$$

Since this equation supposes steady-state creep which was not observed in experiment, the determination of A^p and n has to be accomplished in an arbitrary manner. This is illustrated by the fact that the time dependent curves in Fig. 8 have to be approximated by a horizontal line. The approximations establish following values: $A^p = 1.4 \cdot 10^{-15}$/s and $n = 5.0$. These parameters agree very well with those given by Albrecht and Hunsche (1980) for a temperature of 308 K.

For relaxation with constant strain we obtain from Eq. (39)

$$\dot{\sigma} = -EA^p \left(\frac{\sigma}{\sigma_0}\right)^n. \tag{41}$$

Since the power law supposes relaxation processes to be independent of strain, the stress dependent relaxation rates of Fig. 9 have to be approximated by *one* straight line with the gradient n and the intercept of the ordinate of $A^p \cdot E$ from which E can be calculated. Obviously, the given stress exponent n allows only a very poor and arbitrary approximation because straight lines with a gradient of 5.0 show significant deviations from the test results in any case. Accordingly, Young's modulus E can be chosen in a range of some decades and may become completely unrealistic. For further calculations $E = 20\,000$ MPa is used (Fig. 9).

Hyperbolic Sine Law

The hyperbolic sine creep law can be written as

$$\dot{\varepsilon} = \frac{\dot{\sigma}}{E} + A^{sh} \sinh\left(B^{sh} \frac{\sigma}{\sigma_0}\right). \tag{42}$$

For uniaxial creep and $\exp(2\,B^{sh}\,\sigma/\sigma_0) \gg 1$ the following equation is valid:

$$\dot{\varepsilon} = A^{sh} \sinh\left(B^{sh} \frac{\sigma}{\sigma_0}\right) \approx \frac{A^{sh}}{2} \exp\left(B^{sh} \frac{\sigma}{\sigma_0}\right). \tag{43}$$

This relation yields a straight line in a $\log(\dot{\varepsilon}) - (\sigma/\sigma_0)$-representation from which the parameters A^{sh} and B^{sh} are derived as $A^{sh} = 1.4 \cdot 10^{-12}/\text{s}$ and $B^{sh} = 0.46$. Under corresponding conditions the equation describing uniaxial relaxation is obtained as

$$\dot{\sigma} = -EA^{sh} \sinh\left(B^{sh} \frac{\sigma}{\sigma_0}\right) \approx -\frac{A^{sh}E}{2} \exp\left(B^{sh} \frac{\sigma}{\sigma_0}\right). \tag{44}$$

By approximating the strain dependent experimental curves by one straight line in a $\ln(-\dot{\sigma}) - (\sigma/\sigma_0)$-diagram E can be determined. Due to very poor agreement $E = 20\,000$ MPa is used again (Fig. 9).

7. Arithmetical Simulation of Test Results

A verification of the proposed constitutive law is accomplished by comparing the relaxation and the stress-strain behaviour both with other constitutive laws and with experimental results. Creep behaviour will not be discussed here in detail since the main subject of this work deals with relaxation behaviour. The considerable divergencies of creep curves predicted by steady-state creep laws and real creep behaviour observed in laboratory were already mentioned.

Relaxation Behaviour

As shown above (Fig. 9), the stress dependent stress rates of steady-state creep laws with a given stress exponent n are not able to agree sufficiently with experimental data. Among others this is due to the fact that in contrast to the strain hardening approach steady-state creep laws do not incorporate strain dependency. However, real relaxation behaviour shows a distinct dependency upon strain. This is exemplarily illustrated by Fig. 11, where some relaxation phases of the test shown in Fig. 7 are depicted.

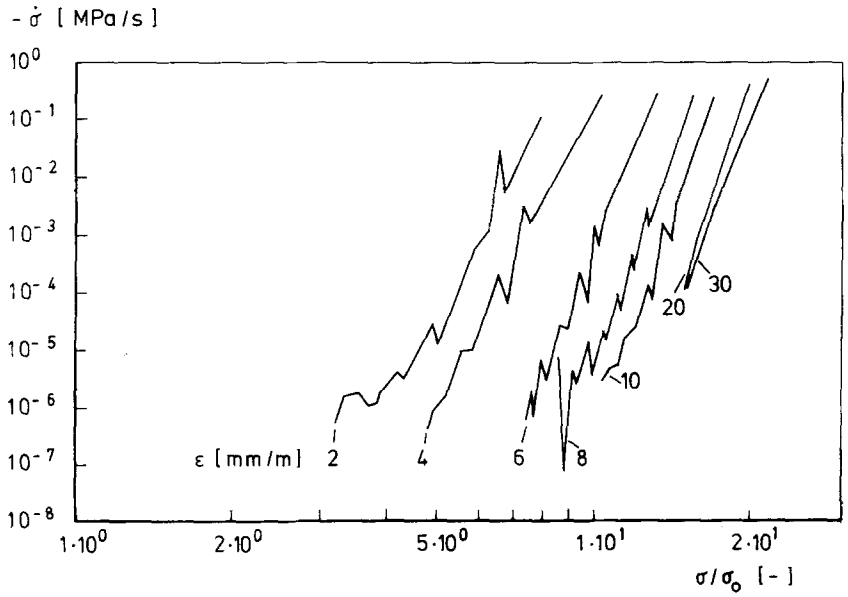

Fig. 11. Stress rate vs. dimensionless stress ($\sigma_0 = 1$ MPa) demonstrating strain dependency of relaxation behaviour

For calculation of time dependent stresses and stress rates by the strain hardening approach the initial stresses $\sigma_a = f(\varepsilon)$ are required. Two representative pairs of values are used: $\sigma_a(\varepsilon = 0.005) = 13$ MPa and $\sigma_a(\varepsilon = 0.020) = 20$ MPa. The relaxation curves of the two steady-state laws are strain independent.

For the power law we obtain from Eq. (39) with the condition $\sigma(t = t_0) = \sigma_a$ the time dependent stresses

$$\sigma = \sigma_a \left[\frac{(t - t_0)}{t_r^p} + 1 \right]^{\frac{1}{1-n}} \tag{45}$$

and the time dependent stress rates

$$\dot{\sigma} = -EA^p \left(\frac{\sigma_a}{\sigma_0}\right)^n \left[\frac{(t-t_0)}{t_r^p} + 1\right]^{\frac{n}{1-n}}, \tag{46}$$

where

$$t_r^p = \frac{\sigma_0}{(n-1)\,EA^p} \left(\frac{\sigma_a}{\sigma_0}\right)^{1-n}. \tag{47}$$

Integration of the hyperbolic sine relaxation function (left part of Eq. (44)) with

$$C_1 = \tanh\left(\frac{B^{sh}\,\sigma_a}{2\,\sigma_0}\right) \tag{48}$$

and

$$t_r^{sh} = \frac{\sigma_0}{A^{sh}E} \tag{49}$$

yields

$$\sigma = -\frac{\sigma_0}{B^{sh}} \ln\left[\frac{1 - C_1 \exp\left(-\dfrac{t-t_0}{t_r^{sh}}\right)}{1 + C_1 \exp\left(-\dfrac{t-t_0}{t_r^{sh}}\right)}\right] \tag{50}$$

and

$$\dot{\sigma} = -\frac{2\,A^{sh}EC_1 \exp\left(-\dfrac{t-t_0}{t_r^{sh}}\right)}{1 - C_1^2 \exp\left(-2\dfrac{t-t_0}{t_r^{sh}}\right)}. \tag{51}$$

Figure 12 shows the measured time dependent stress rates (plotted as hatched domain) in comparison with curves calculated by Eqs. (35), (46) and (51). It is clearly seen that the real material behaviour is described excellently by the strain hardening approach whereby in accordance with the observations the strain dependency is not strongly marked. On the contrary, the power law as well as the hyperbolic sine law exhibit distinct deviations from real material behaviour.

This is confirmed by Fig. 13 where the time dependent stress is shown. Stress relaxation described by the hyperbolic sine law (Eq. (50)) is nearly completely finished in the not-too-distant future. This behaviour seems to be very unrealistic. On the contrary, long-time relaxation may be simulated sufficiently by the power law (Eq. (45)). However, both steady-state creep laws are not able to describe the initial strong stress decrease and no improvement can be achieved by variation of material parameters within the limits of realistic values.

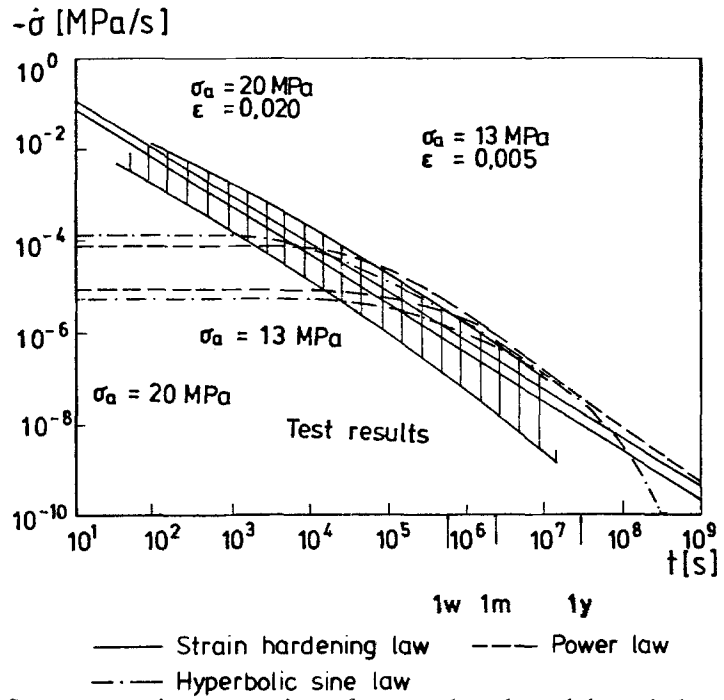

Fig. 12. Stress rate vs. time: comparison of measured results and theoretical predictions

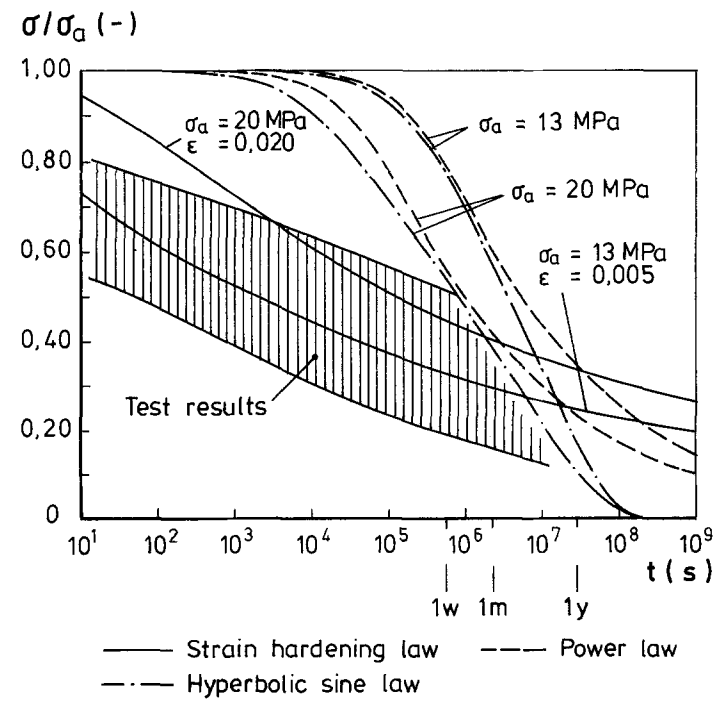

Fig. 13. Dimensionless stress vs. time: comparison of measured results and theoretical predictions

Stress-Strain-Behaviour at Constant Strain Rates and Constant Stress Rates

By inserting $B=\beta$ and $D=\delta$ into Eq. (27), a constant strain rate test with $\dot{\varepsilon}=\dot{\varepsilon}_c=\text{const.}$ is described by the strain hardening approach as follows:

$$\dot{\sigma}=\frac{A}{\alpha}\dot{\varepsilon}_c-A\,\dot{\varepsilon}_c^{-B}\left(\frac{\sigma}{\sigma_0}\right)^D t^{-B}. \tag{52}$$

Accordingly, a constant stress rate test is given by

$$\dot{\varepsilon}=\frac{\alpha}{A}\dot{\sigma}_c+\alpha\,\varepsilon^{-\beta}\,t^{\delta}\left(\frac{\dot{\sigma}_c}{\sigma_0}\right)^{\delta}. \tag{53}$$

These equations require numerical solutions.

A steady-state creep law basing on Eq. (19) may be rewritten for a constant strain rate $\dot{\varepsilon}_c$ using the chain rule as

$$\left(1-\frac{1}{E}\frac{\delta\sigma}{\delta\varepsilon}\right)\dot{\varepsilon}_c=c\,(\sigma) \tag{54}$$

(Cernocky and Krempl, 1980, e. g.). Since this equation must be valid for all $\dot{\varepsilon}_c$ there must be

$$\frac{\delta\sigma}{\delta\varepsilon}=E \tag{55}$$

for $\sigma=0$, where $c\,(\sigma=0)=0$. This means that the material initially behaves linear-elastically independently of the strain rate. If $c\,(\sigma)$ reaches a value $c\,(\sigma)=\dot{\varepsilon}_c$ there is

$$\frac{\delta\sigma}{\delta\varepsilon}=0. \tag{56}$$

Accordingly, at a certain stress the slope of the stress-strain-curve becomes zero. The corresponding strain rate dependent stress which cannot be exceeded is given by

$$\sigma=\sigma_0\left(\frac{\dot{\varepsilon}_c}{A^p}\right)^{\frac{1}{n}} \tag{57}$$

for the power law and by

$$\sigma=\frac{\sigma_0}{B^{sh}}\operatorname{arsinh}\left(\frac{\dot{\varepsilon}_c}{A^{sh}}\right) \tag{58}$$

for the hyperbolic sine law.

The calculated σ-values compared with the measured stress-strain-curves for constant strain rate ($\dot{\varepsilon}=4\cdot10^{-5}/\text{s}$) are shown in Fig. 14. The curve basing on the strain hardening law is lying exactly within the scattering of the test results. On the contrary, steady-state creep laws show significant deviations from real behaviour. They describe almost linear-elastic/ideal-plastic behaviour whereby absolutely unrealistic stresses of about 40 MPa for the power law and more than 120 MPa for the hyperbolic sine law are reached.

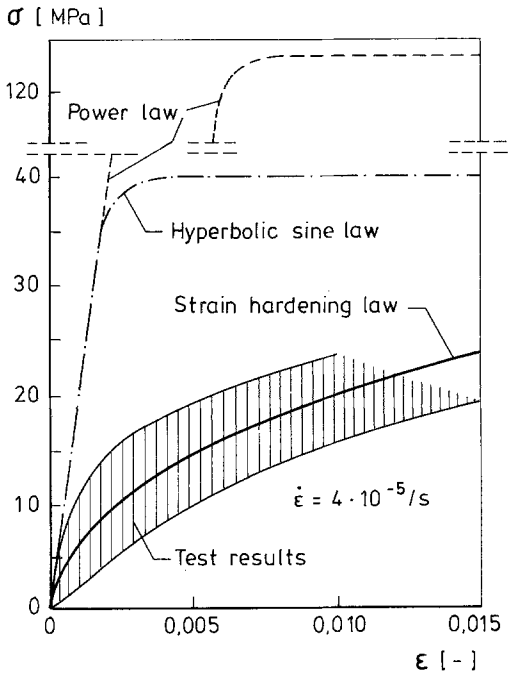

Fig. 14. Stress vs. strain: comparison of measured results and theoretical predictions

8. Conclusions

It was shown that conventional constitutive equations for rock salt have considerable imperfections and hence are not able to simulate real material behaviour sufficiently. Moreover, only few of the great number of existing constitutive laws could be carried into practice. For instance, essence and purpose of equations incorporating up to 20 parameters or of those with an extremely restricted range of application seems to be doubtful.

A decisive lack in salt rock research was the negligence of relaxation characteristics. Among others this was due to the opinion according to which relaxation behaviour can be unambiguously deduced from creep behaviour with the help of atomic process theories or by rheological models. However, this hypothesis is mainly disproved by the results of the relaxation tests described above.

The use of steady-state creep laws is often justified by the observation that long-time creep and relaxation behaviour sufficiently show agreement with test results whereas initial behaviour is of no importance for practical purposes. Indeed, the long-time relaxation behaviour can be described fairly good by the power law, as shown by Fig. 13. However, extremely restrictive conditions, as given in creep or relaxation tests, cannot be found in situ. Hence, the quality of constitutive equations may not be estimated on the basis of results of a single test type. Constant strain rate and constant stress rate tests for example require the co-operation of creep and

relaxation processes and in this respect represent in situ conditions much better than creep or relaxation tests. But just the post-calculation of these tests show a significant superiority of the strain hardening law compared with steady-state creep laws.

Acknowledgement

The works were performed at the Institute for Soil Mechanics and Rock Mechanics of the University of Karlsruhe, Germany. I wish to thank all co-workers of the Division for Rock Mechanics for the support and helpful discussions, especially Professor Dr.-Ing. O. Natau, chair of rock mechanics, Professor Dr. rer. nat. G. Borm and Mr. K. (Felix) Balthasar.

References

Albrecht, H., Hunsche, U. (1980): Gebirgsmechanische Aspekte bei der Endlagerung radioaktiver Abfälle in Salzdiapiren unter besonderer Berücksichtigung des Fließverhaltens von Steinsalz. Fortschr. Miner. 58, 212—247.

Balthasar, K., Haupt, M., Lempp, C., Natau, O. (1987): Stress relaxation behaviour of rock salt: Comparison of in situ measurements and laboratory test results. Proc. 6th Int. Congr. Rock Mech., Montreal.

Becker, E., Bürger, W. (1975): Kontinuumsmechanik. B. G. Teubner, Stuttgart.

Cernocky, E. P., Krempl, E. (1979): A non-linear uniaxial integral constitutive equation incorporating rate effects, creep and relaxation. Int. J. Nonlinear Mech. 14, 183—203.

Cernocky, E. P., Krempl, E. (1980): A theory of viscoplasticity based on infinitesimal total strain. Acta Mechanica 36, 263—289.

Dreyer, W. (1967): Die Festigkeitseigenschaften natürlicher Gesteine insbesondere der Salz- und Karbongesteine. Clausthaler Hefte zur Lagerstättenkunde und Geochemie der mineralischen Rohstoffe 5.

Fernandez, G., Hendron, A. J. (1984): Interpretation of a long-term in situ borehole test in a deep salt formation. Bull. of the Ass. of Eng. Geol. 21, 23—38.

Frost, H. J., Ashby, M. F. (1984): Deformation-mechanism maps. Pergamon Press, Oxford.

Haupt, M. (1988): Entwicklung eines Stoffgesetzes für Steinsalz auf der Basis von Kriech- und Relaxationsversuchen. Veröff. Inst. für Bodenmech. und Felsmech. der Universität Karlsruhe.

Heard, H. C. (1972): Steady-state flow in polycrystalline halite at pressure of 2 kilobars. Flow and Fracture of Rocks, Am. Geophys. Union, 191—209.

Höfer, K.-H., Knoll, P. (1971): Investigations into the mechanism of creep deformation in carnallitite and practical applications. Int. J. Rock Mech. Min. Sci. 8, 61—73.

Le Comte, P. (1965): Creep in rock salt. J. of Geology 73, 469—484.

Liu, M. C. M., Krempl, E. (1979): A uniaxial viscoplastic model based on total strain and overstress. J. Mech. Phys. Solids 27, 377—391.

Lomenick, T. F., Bradshaw, R. L. (1969): Deformation of rock salt in openings mined for the disposal of radioactive wastes. Rock Mechanics 1 (1), 5—29.

McCartney, L. N. (1976): No time — gentlemen please! Philos. Mag. 33, 689—695.

McVetty, P. G. (1943): Creep of metals at elevated temperatures — the hyperbolic-sine relation between stress and creep rate. Transactions of the A. S. M. E., 761—769.

Menzel, W., Schreiner, W. (1975): Das Festigkeits- und Verformungsverhalten von Carnallitit als Grundlage für die Standsicherheitsbewertung von Grubenbauten. Neue Bergbautechnik 5, 451—457.

Menzel, W., Schreiner, W. (1977): Zum geomechanischen Verhalten von Steinsalz verschiedener Lagerstätten der DDR. Teil II: Das Verformungsverhalten. Neue Bergbautechnik 7, 565—574.

Mott, N. F. (1953): A theory of work-hardening of metals — II: Flow without slip-lines, recovery and creep. Philos. Mag. 44, 742—765.

Munson, D. E., Dawson, P. R. (1984): Salt constitutive modeling using mechanism maps. First Conf. Mech. Beh. of Salt, Pennsylvania State University, University Park.

Nadai, A. (1938): The influence of time upon creep, the hyperbolic sine creep law. Timoshenko Anniversary Volume, Macmillan, New York, 155—170.

Nicolas, A., Poirier, J. P. (19769: Crystalline plasticity and solid flow in metamorphic rocks. J. Wiley, New York.

Odqvist, F. K. G., Hult, J. (1962): Kriechfestigkeit metallischer Werkstoffe. Springer, Berlin Göttingen Heidelberg.

Poirier, J. P. (1985): Creep of crystals. Cambridge University Press, Cambridge.

Prandtl, L. (1928): Ein Gedankenmodell zur kinematischen Theorie der festen Körper. Zeitschr. f. angew. Mathem. u. Mechanik 8, 85—106.

Reiner, M. (1968): Rheologie in elementarer Darstellung. Carl Hanser Verlag, München.

Rivlin, R. S. (1970): Red herrings and sundry unidentified fish in non-linear continuum mechanics. Inelastic behaviour of solids. McGraw-Hill, New York.

Serata, S. (1968): Application of continuum mechanics to design of deep potash mines in Canada. Int. J. Rock Mech. Min. Sci. 5, 293—314.

Thoms, R. L., Char, C. V., Bergeron, W. J. (1973): Finite element analysis of rock-salt pillar models. Proc. 14th Symp. Rock Mech., Pennsylvania, 392—408.

Verrall, R. A., Fields, R. J., Ashby, M. F. (1977): Deformation-mechanism maps for LiF and NaCl. J. of the Am. Ceramic Soc. 60, 211—216.

Wagner, R. A. (1982): An evaluation of a finite element simulation of the thermomechanical response of dome salt to an emplaced heat source. Int. Symp. Num. Models in Geomech., Zurich, 499—507.

Wawersik, W. R. (1985): Determination of steady state creep rates and activation parameters for rock salt. Spec. Techn. Publ. 869, Am. Soc. for Testing and Materials, Philadelphia.

Wawersik, W. R., Herrmann, W., Montgomery, S. T., Lauson, H. S. (1984): Excavation design in rock salt — laboratory experiments, material modeling and validations. Proc. ISRM-Symp. Aachen, 1345—1356.

Winkel, B. V., Gerstle, K. H., Ko, H. Y. (1972): Analysis of time-dependent deformations of openings in salt media. Int. J. Rock Mech. Min. Sci. 9, 249—260.

Author's address: Dr. M. Haupt, Philipp Holzmann AG., Technical Department, Taunusanlage 1, D-W-6000 Frankfurt, Federal Republic of Germany.